JOC The Journal of Organic Chemistry

Article

pubs.acs.org/joc

Spectroscopic and Computational Investigations of The Thermodynamics of Boronate Ester and Diazaborole Self-Assembly

Alexander R. Goldberg and Brian H. Northrop*

Department of Chemistry, Wesleyan University, Middletown, Connecticut 06459, United States

Supporting Information

ABSTRACT: The solution phase self-assembly of boronate esters, diazaboroles, oxathiaboroles, and dithiaboroles from the condensation of arylboronic acids with aromatic diol, diamine, hydroxythiol, and dithiol compounds in chloroform has been investigated by ^{1}H NMR spectroscopy and computational methods. Six arylboronic acids were included in the investigations with each boronic acid varying in the substituent at its 4-position. Both computational and experimental results show that the para-substituent of the arylboronic acid does not significantly influence the favorability of forming a condensation product with a given organic donor. The type of donor, however, greatly influences the favorability of self-assembly. ^{1}H NMR spectroscopy indicates that condensation reactions between arylboronic acids and catechol to give boronate esters are the most favored thermodynamically, followed by diazaborole formation. Computational investigations support this conclusion. Neither oxathiaboroles nor dithiaboroles form spontaneously at equilibrium in chloroform at room temperature. Computational results suggest that the effect of borylation on the frontier orbitals of each donor helps to explain differences in the favorability of their condensation reactions with arylboronic acids. The results can inform the use of boronic acids as they are increasingly utilized in the dynamic self-assembly of organic materials and as components in dynamic combinatorial libraries.

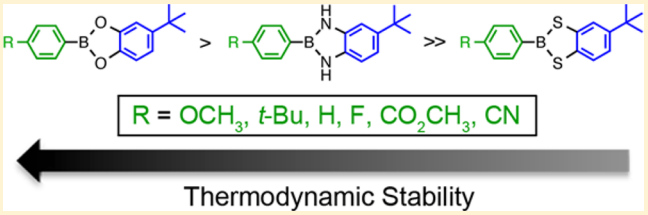

INTRODUCTION

Dynamic covalent reactions involving boronic acids have long been recognized for their utility in the design of receptors and sensors for compounds such as saccharides[1] and anions.[2] More recently the self-assembly of boronic acids has proven to be a powerful means of preparing complex macrocycles,[3] cages,[4] and functional polymers[5] and has given rise to the field of covalent organic frameworks (COFs).[6] Much of the unique and advantageous chemistry of boronic acids arises from the low valency and the empty p orbital of their constituent boron atom(s), which enables them to accept electron density from a wide variety of species. The condensation of boronic acids with 1,2-diols results in the formation of cyclic boronate esters (Scheme 1a), while the self-condensation of boronic acids gives boroxine anhydrides (Scheme 1b).[7−11] Both boronate ester and boroxine anhydride formations are thermodynamically reversible despite their formation of strong B−O covalent bonds and the entropic favorability of liberating two and three molecules of water, respectively. The equilibria shown in Scheme 1 can be driven toward products by a variety of means (azeotropic removal of water, dehydrating agents, product precipitation, etc.), however the hydrolysis of boronate esters and boroxine anhydrides is a common concern and varies significantly with the functionality of boronic acid and diol components as well as the choice of solvent.[7]

The self-assembly of boronate ester and boroxine anhydride species in aqueous solutions has been thoroughly investigated.[9,12−15] By contrast, few investigations of the thermodynamics and dynamic assembly processes of boronic acids in nonaqueous solutions have been reported in the literature.[16−18] This is despite over two decades of broad interest in the use of boronic acids in synthesis, self-assembly, and materials chemistry.[8,9] It is known that the favorability of forming esters and boroxines from boronic acids depends on the functionality of the acid, the solvent, and the presence of coordinating donors. Many boronic acids readily dehydrate in nonpolar solvents (e.g., CH_2Cl_2 and $CHCl_3$) to form their less polar boroxine analogues. Tokunaga and co-workers have inves-

Scheme 1. General Representation of (a) Boronate Ester Formation from the Reversible Condensation of Boronic Acids with Organic Diols and of (b) Boroxine Anhydride Formation from the Self-Condensation of Three Equivalents of Boronic Acids

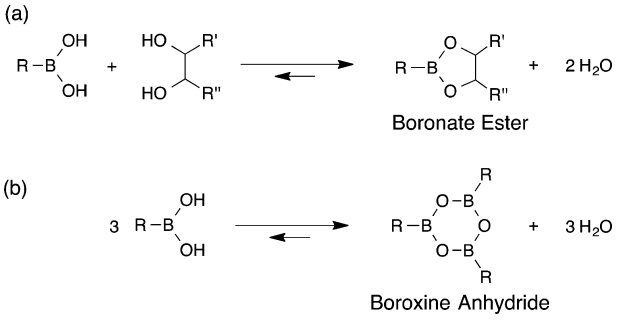

Received: November 5, 2015

DOI: 10.1021/acs.joc.5b02548
J. Org. Chem. XXXX, XXX, XXX−XXX

tigated the free energy of boroxine formation from para-substituted aryl boronic acids in chloroform and found the self-condensation to be entropically driven and generally endergonic.[17] Electron-donating substituents have been shown to increase the favorability of boroxine formation by decreasing the electrophilicity of boron, thereby decreasing their susceptibility to hydrolysis. Electron-withdrawing substitutents have the opposite effect. Computational investigations by Kua and Iovine generally support the experimental observations.[19] Dehydration of boronic acids to boroxines is facilitated by the presence of nitrogen donor compounds (e.g., tertiary amines or pyridine), resulting in the formation of boroxine donor adducts that have been found to be thermodynamically more favorable than uncoordinated boroxines.[10,19−24] In fact, the ligand-facilitated trimerization of boronic acids can be used to promote the formation of boroxines.

The formation of boronate esters from the condensation of boronic acids with diols is also influenced by the nature of the solvent and the functionality of the starting compounds. As with boroxines, boronate esters are less polar than their starting boronic acids, and this difference in polarity can be used to shift their equilibria toward esters in nonpolar solvents. The stability of boronate esters to hydrolysis is highly influenced by the nature of their component diols. Sterically hindered boronates (e.g., pinacolboranes) are known to be relatively stable in protic solvents, while less hindered boronates (e.g., ethylene glycol esters) are quite susceptible to hydrolysis.[7] As noted earlier, condensations of arylboronic acids and catechol derivatives have been recently and widely used in the dynamic covalent assembly of boronate ester-based organic materials, such as boronate ester macromolecules[5] and COFs.[6] The majority of such organic materials are prepared using organic solvents. Despite this growing area of research, and to the best of our knowledge, no experimental or computational studies focusing on the thermodynamics of boronate ester self-assembly in nonaqueous environments have been reported.

Similarly, very little is known of the thermodynamics of related dynamic assembly processes between boronic acids and *ortho*-phenylenediamines to give diazaboroles.[25] The first example of a diazaborole condensation, reported by Letsinger over 50 years ago, was formed by the reaction of *ortho*-phenylenediamine with the ethyl tartarate ester of phenylboronic acid.[26] More recently diazaboroles have been shown to function as blue emissive materials,[27] photoluminescent polymers,[28] and p-type semiconductors in organic field-effect transistors.[29] Diazaboroles are known to hydrolyze rapidly in mildly acidic conditions, however they are generally stable in neutral solutions. Dithiaboroles, another class of related boron heterocycles, have been reported, though they are typically synthesized from 2-chloro-1,3,2-dithiaborole derivatives[30−32] rather than through the condensation of dithiols with boronic acids. A more quantitative understanding of the influence of boronic acid and organic donor functionality on the favorability of their self-assembly processes will likely (i) provide access to new boron-based materials from dynamic covalent and dynamic combinatorial assembly of different secondary building units and (ii) enable predictable exchange processes when thermodynamics sufficiently favor the formation of one type of assembly over another. The design of new boronic acid-derived sensors, polymers, COFs, and other functional materials will benefit from such an increased understanding of the thermodynamics of their assembly processes.

Herein we present combined spectroscopic and computational investigations of the self-assembly of para-substituted aryl boronic acids with a series of aryl donors bearing alcohol, amine, and thiol functionalities. We find that the para-substituent of the aryl boronic acid does not significantly influence the thermodynamics of their self-assembly with the different organic donors. The functionality of the organic donor, by contrast, is found to influence the favorability of forming stable condensation products considerably.

RESULTS AND DISCUSSION

Shown in Figure 1a are the six phenylboronic acids investigated in the present study: 4-methoxyphenylboronic acid (**1**), 4-*tert*-butylphenylboronic acid (**2**), phenylboronic acid (**3**), 4-fluorophenylboronic acid (**4**), 4-methoxycarbonylphenylboronic acid (**5**), and 4-cyanophenylboronic acid (**6**). Para-substituted arylboronic acids were chosen because experimental investigations have demonstrated that ortho-substituted boronic acids are less favored to assemble into boroxines or boronate esters, largely due to steric effects.[7] Para-substituted acids allow the influence of electronic effects on assembly processes to be studied independent of the size of a given substituent. Furthermore, the symmetry of para-substituted acids aids significantly in investigating their assembly processes by ^{1}H NMR spectroscopy. The chemical structures of four different organic donors are shown in Figure 1b: 4-*tert*-butylcatechol (**7**), 4-*tert*-butyl-*ortho*-phenylenediamine (**8**), 2-hydroxybenzenethiol (**9**), and toluene-3,4-dithiol (**10**).

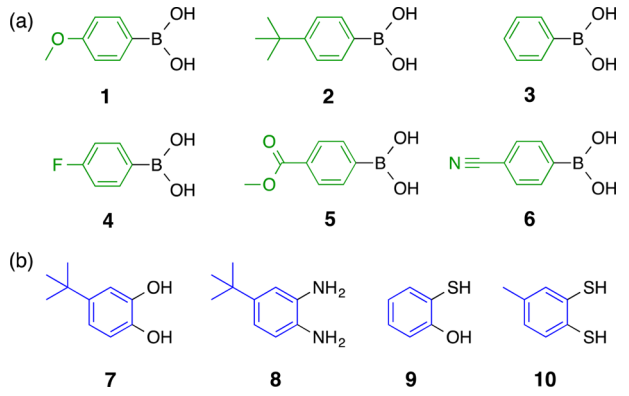

Figure 1. Chemical structures of the (a) aryl boronic acids and (b) organic donor compounds investigated in the current study.

Aryl boronic acids and aryl organic donors were chosen because of their prevalent use in the design, synthesis, and self-assembly of polymeric materials and COFs. Donation of electron density from oxygen to boron in boronate esters can increase their stability by disfavoring hydrolysis. In the case of catechol derivatives, however, lone pair electrons of catechol oxygen atoms are also able to conjugate with the aromatic ring, weakening their interaction with boron. Catechol-based boronate esters are therefore more susceptible to hydrolysis than, for example, pinacolboranes. This hydrolytic susceptibility is often considered a favorable attribute in the context of dynamic covalent self-assembly[33] where readily reversible covalent bond formation is necessary to provide a means of error correction en route to the most thermodynamically stable structure(s). The role that similar electronic effects play in the thermodynamic stability of diazaboroles and dithiaboroles is currently unknown. Amine- and thiol-functionalized donors **8**−

DOI: 10.1021/acs.joc.5b02548
J. Org. Chem. XXXX, XXX, XXX−XXX

10 were therefore chosen to gain insight into the stability of their assemblies with boronic acids **1**−**6**. Investigations of donors beyond catechol also open prospects for elucidating new exchange processes, constructing new dynamic combinatorial libraries, and developing routes to new diazaborole and dithiaborole materials.

To evaluate the thermodynamics of boronate ester self-assembly, we used a combination of experimental, spectroscopic, and computational analysis. Experimentally, pairwise combinations of boronic acids **1**−**6** and organic donors **7**−**10** were mixed in 1:1 molar ratios in $CDCl_3$ at room temperature and allowed to reach equilibrium. The extent of assembly formation was then determined by the relative integration values of signals corresponding to acid, ester, and, in some cases, boroxine species by ^{1}H NMR spectroscopy. In conjunction with spectroscopic analysis, the energetics of boronate ester and boroxine formation were studied computationally. The use of a combination of computational and spectroscopic investigations was motivated by the desire to benchmark different computational methods against experimental results and, ideally, to elucidate the electronic and/or structural factors that underlie differences in the thermodynamics of boronate ester, diazaborole, and dithiaborole formation.

^{1}H NMR Spectroscopy. In principle, boronic acids **1**−**6** are able to condense with donors **7**−**10** to give boronate esters (**11a**−**f**), diazaboroles (**12a**−**f**), oxathiaboroles (**13a**−**f**), and dithiaboroles (**14a**−**f**), as shown in Scheme 2. Equimolar solutions of each boronic acid and each donor were mixed in $CDCl_3$ (0.05 M) and allowed to reach equilibrium at room temperature. Particular care was taken to dry all starting materials and $CDCl_3$ given the role that water plays in the dynamic equilibrium of boronic acid condensation reactions (full details are provided in the Computational and Experimental Methods section). While assembly kinetics were not a focus of the current investigation, it was readily observed that the room temperature condensation of boronate esters **11a**−**f** is more rapid than the condensation of diazaboroles **12a**−**f** under identical conditions. ^{1}H NMR spectra of mixtures containing any of the six boronic acids and *tert*-butylcatechol (**7**) showed nearly complete product formation within 30 min of mixing, and no changes in the relative integrations of proton signals could be observed after approximately 4 h. ^{1}H NMR spectra of equimolar mixtures of boronic acids **1**−**6** and *tert*-butyl-*ortho*-phenylenediamine (**8**) were observed to evolve more progressively over the course of approximately 24 h, after which no appreciable change could be observed. Mixtures containing boronic acids **1**−**6** and either hydroxybenzenethiol (**9**) or toluene-3,4-dithiol (**10**) showed no discernible oxathiaborole or dithiaborole formation. It could be concluded from ^{1}H NMR spectroscopy alone that the formation of oxathiaboroles (**13**) and dithiaboroles (**14**) by the condensation of aryl boronic acids with **9** or **10** is thermodynamically unfavored under these conditions, though similar structures have been prepared by the reaction of hydroxythiol and dithiol compounds with dichlorophenylboranes[34] or by the aforementioned routes using haloboranes.[31]

Scheme 2. Dynamic Covalent Exchange Reactions between Phenylboronic Acids 1−6 and Aryl Donors 7−10 Investigated by ^{1}H NMR Spectroscopy

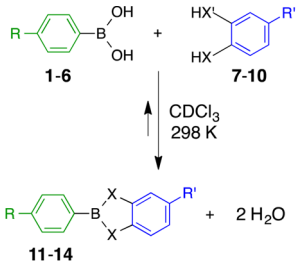

	11a-f	12a-f	13a-f	14a-f
X	O	NH	O	S
X'	O	NH	S	S
R'	*t*-Bu	*t*-Bu	H	Me

R =	OMe	*t*-Bu	H	F	CO_2Me	CN
	a	b	c	d	e	f

Relative integrations of ^{1}H NMR spectroscopic signals were used to calculate equilibrium constants (K_{eq}) and free energies (ΔG°) for the condensation reactions between boronic acids **1**−**6** with catechol **7** and *ortho*-phenylenediamine **8**. Assignments of boronic acid, boroxine anhydride, and boronate or diazaborole species were made by comparison to pure samples of boroxines and condensation products **11a**−**f** and **12a**−**f**. For most compounds, the singlet of the 4-*tert*-butyl group of **7** and **8** was found to be particularly diagnostic as it appears at 1.26 ppm for the free donor species but undergoes a downfield shift to 1.35−1.37 ppm (esters **11a**−**f**) or 1.36−1.38 ppm (diazaboroles **12a**−**f**) upon condensation with boronic acids **1**−**6**. Furthermore, the *tert*-butyl singlets of assembled and unassembled species, integrating to 9 symmetry equivalent protons, provide the greatest signal-to-noise of all spectroscopic signals and therefore provide the most reliable means of evaluating the percentages of product formation. Assemblies containing *tert*-butylphenylboronic acid **2** were the exception because *tert*-butyl peaks corresponding to several species (i.e., unassembled **7** or **8**, unassembled **2**, ester or diazaborole products **11b** or **12b**, and the boroxine anhydride of **2**) overlap in their equilibrated ^{1}H NMR spectra. When possible, calculated ratios of condensation products were corroborated by the integration of diagnostic signals in the aromatic region of each spectrum. Figure 2 shows a representative example corresponding to the equilibrium between 4-cyanophenylboronic acid **6**, *tert*-butylcatechol **7**, and their condensation product boronate ester **11f**. Collected in Table 1 are the calculated equilibrium constants and free energies of condensation reactions between each of the boronic acids shown in Figure 1a and donors **7**−**10**.

Boronic acids functionalized with electron-withdrawing groups, namely 4-methylcarbonylphenyl boronic acid (**5**) and 4-cyanophenylboronic acid (**6**), gave the lowest yields of boronate ester formation at equilibrium: 94% of **11e** and 92% of **11f**. The remaining four boronic acids gave boronate esters **11a**−**d** in 96−97% yield, which may be considered identical within experimental error. Overall the formation of all six boronate esters is predicted to be exergonic, with reaction free energies ranging from ΔG° = −1.1 to −2.5 kcal/mol. The results summarized in Table 1 suggest that electron-rich boronic acids form more thermodynamically stable boronate ester assemblies with catechol **7**, while acids bearing electron-withdrawing groups form less stable boronate esters, however the differences in yield, K_{eq}, and ΔG° are quite small considering the large differences in Hammett parameters among the six functional groups investigated: σ_{para} ranges from −0.27 (methoxy) to +0.66 (cyano). Overall, all six of the

DOI: 10.1021/acs.joc.5b02548
J. Org. Chem. XXXX, XXX, XXX−XXX

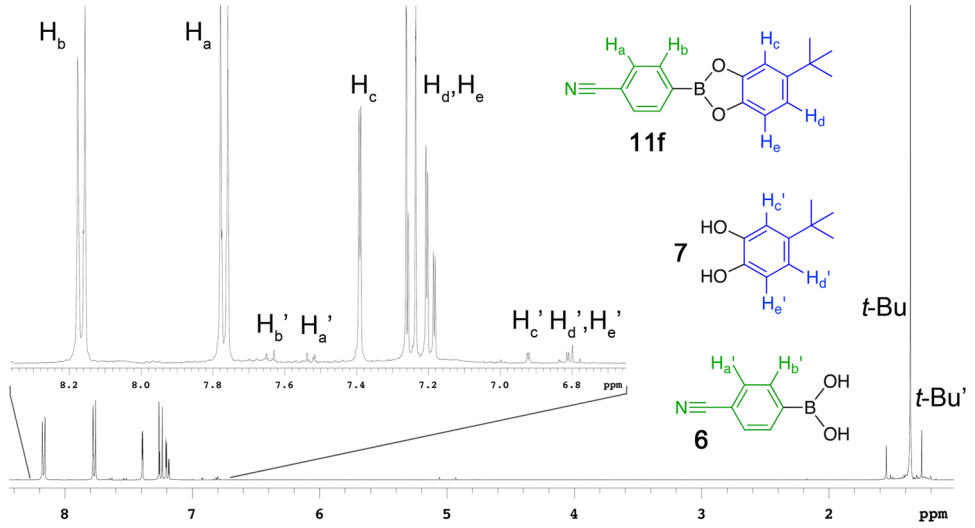

Figure 2. Example equilibrated mixture of 4-cyanophenylboronic acid (**6**), 4-*tert*-butyl catechol (7), and their corresponding boronate ester **11f** (0.05 M in $CDCl_3$, 298 K, 300 MHz). Signals of both unassembled and assembled species are observed and were used for the calculation of the equilibrium constant (K_{eq}) and condensation free energy ($\Delta G°$) of boronate ester formation. Full ^{1}H NMR spectra for all condensations are provided in Figures S7−S18 of the Supporting Information.

Table 1. Equilibrium Constants and Corresponding Reaction Free Energies for the Formation of Boronate Esters 11a−f and Diazaboroles 12a−f as Determined from ^{1}H NMR Spectroscopy at 25 °C[a]

		R[b]	% product	K_{eq}[c]	$\Delta G°$[d]
11	**a**	OMe	97	44.7	−2.3
	b	*t*-Bu	96	24.9	−1.9
	c	H	97	75.5	−2.5
	d	F	96	32.9	−2.1
	e	CO_2Me	94	10.8	−1.4
	f	CN	92	6.4	−1.1
12	**a**	OMe	33	3.84×10^{-3}	3.3
	b	*t*-Bu	44	1.37×10^{-2}	2.5
	c	H	30	2.59×10^{-3}	3.5
	d	F	30	2.61×10^{-3}	3.5
	e	CO_2Me	42	1.07×10^{-2}	2.7
	f	CN	42	1.10×10^{-3}	2.7

[a]The dynamic covalent assembly of oxathiaboroles (**13a−f**) and dithiaboroles (**14a−f**) as outlined in Scheme 2 was not observed. Complete details and ^{1}H NMR spectra used to determine K_{eq} contained in the Supporting Information. [b]R indicates the substituent at the para-position of the boronic acid. [c]K_{eq} = [ester][H_2O]^2/([acid][donor]). [d]kcal/mol.

arylboronic acids investigated readily assemble with catechol **7** in chloroform, and the equilibrium formation of boronate esters **11a−f** lies heavily toward products (>90% assembly formation).

The dynamic assembly of *ortho*-phenylenediamine **8** with boronic acids **1−6** results in significantly less diazaborole formation as compared to boronate ester formation. Substantial quantities of uncondensed boronic acid and diamine species can be observed in the ^{1}H NMR spectra of each equilibrated mixture. Diazaborole formation was found to be endergonic in all cases ($\Delta G°$ = 2.5−3.5 kcal/mol) with each mixture resulting in <50% product formation at equilibrium for 0.05 M solutions. The range of reaction free energies observed for the formation of diazaboroles **12a−f** ($\Delta\Delta G°$ = 1.0 kcal/mol) is somewhat narrower than that for the formation of boronate esters **11a−f** ($\Delta\Delta G°$ = 1.4 kcal/mol), again suggesting that the para-substituent of boronic acids **1−6** plays a relatively minor role in determining the thermodynamic favorability of assembly formation. It is interesting to note that the small influence the para-substituent has on diazaborole formation is the opposite of its influence in boronate ester formation. That is, the assembly of *ortho*-phenylenediamine **8** with boronic acids **5** and **6**, which bear electron-withdrawing groups, is found to be slightly more favored than the assembly of electron-rich boronic acids with **8**. Looking at the ^{1}H NMR spectra of equilibrated mixtures of diazaboroles **12a−f** provides some insight into why this may be the case. Equilibrium mixtures of diazaboroles **12a−c** contain substantial quantities of boroxine anhydride and little to no free boronic acid species (see Figures S13−S15 of the Supporting Information). By contrast no boroxine species are observed in the equilibrated mixtures of diazaboroles **12d−f**. These results suggest that boroxine anhydride formation may compete with diazaborole formation when electron-rich arylboronic acids (e.g., **1** and **2**) are used, while boroxine formation is not favored in the case of boronic acids bearing electron-withdrawing groups (e.g., **4−6**). As mentioned earlier, electron-poor arylboroxine anhydrides are known to hydrolyze more readily than electron-rich boroxine species. The competitive formation of broxine species will decrease the extent of diazaborole formation at equilibrium, potentially explaining why the formation of electron-poor diazaboroles is more favored than electron-rich diazaboroles. The same is likely true in the equilibrium formation of boronate esters **11a−f**, however the influence of boroxine formation is less pronounced given the greater favorability of boronate formation relative to diazaborole formation.

Collectively, the spectroscopic results summarized above indicate that the para-substituent of boronic acids **1−6** plays a relatively small role in influencing the thermodynamics of boronate ester or diazaborole formation. The choice of donor, however, significantly influences the favorability of assembly formation. All else being equal (boronic acid, concentration, temperature, and solvent), boronate ester formation is favored over diazaborole formation by 3.9−6.0 kcal/mol. Furthermore, as noted above, no evidence of the self-assembly of

DOI: 10.1021/acs.joc.5b02548
J. Org. Chem. XXXX, XXX, XXX−XXX

oxathiaboroles or dithiaboroles could be observed by ^{1}H NMR spectroscopy. To gain additional insight into the influence of both the organic donor and para-substituted boronic acid components on the favorability of boronate ester and diazaborole formation as well as the unfavorability of oxathiaborole and dithiaborole formation, we explored the thermodynamics of their assembly using computational methods.

Computational Investigations. The energetics of forming condensation products **11**−**14** were studied at four levels of theory, in particular: B3LYP/6-311+G(d,p),[35] M06-2X/6-31+G(d,p),[36] CBS-QB3,[37] and MP2/aug-cc-pVDZ.[38,39] Several computational investigations of boronic acid-derived assemblies have been carried out previously using a variety of theoretical methods.[24,40−43] However, investigations of the thermodynamics of boronate ester, diazaborole, or dithiaborole self-assembly in nonaqueous solutions have not yet been reported. Kua has previously investigated the thermodynamics of boroxine formation and their amine adducts at the B3LYP level, providing insight into the influence of para-substitution and solvent on boroxine and boroxine−amine complex formation.[24a,c] Bock and co-workers, however, have cautioned against the use of B3LYP to quantitatively describe boroxine thermochemistry,[40] recommending MP2 as a more suitable method. B3LYP was still included in the current study to investigate its applicability to modeling boronate thermochemistry and because it is capable of handling large chemical systems. The M06-2X functional has been shown to be broadly applicable for modeling main-group thermochemistry,[36,44] noncovalent interactions,[45] and excited-state chemistry.[46] Furthermore, the M06-2X functional allows for large systems to be handled at reasonable computational cost, making it a good candidate for modeling boronate and boroxine chemistry. CBS-QB3 has been widely shown to give high-accuracy thermochemical results,[47] though calculations at both the CBS-QB3 and MP2 levels have high computational cost. Independent of the method chosen, computational studies have highlighted[41] the need to include diffuse functions to appropriately describe changes in bonding upon boronic acid self-assembly. Basis sets containing diffuse functions were therefore utilized for all levels of theory.

The three most favored conformations of arylboronic acids **1**−**6**, which differ in the relative orientations of their two hydroxyl groups, are shown in Figure 3. All four levels of theory

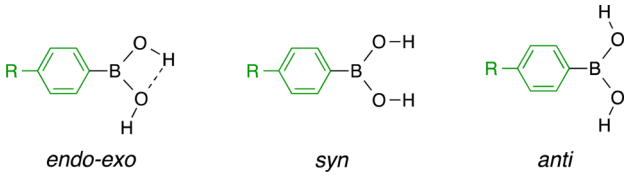

Figure 3. Relative conformations of the three lowest free energy structures of boronic acids **1**−**6**: endo−exo, syn, and anti. The dashed line present in the endo−exo conformation indicates an intramolecular O−H···O hydrogen bond.

predict the endo−exo conformation to be the most favored, as may be expected given that it is the only conformation that allows for the formation of an intramolecular hydrogen bond. *Syn* conformers of **1**−**6** are predicted to be slightly less stable than endo−exo global minima by 0.7−1.3 kcal/mol, while the anti conformers are 2.4−3.0 kcal/mol less stable (Table 2) at the M06-2X/6-31+G(d,p) level of theory. Results at the B3LYP, CBS-QB3, and MP2 levels give the same trend (see Table S1 of the Supporting Information), and overall results are in line with earlier computational studies of aliphatic boronic acids.[40,41,48] The nature of the para-substituent has a small but discernible influence on the structures of arylboronic acids **1**−**6**. For example, the O−H···O intramolecular hydrogen bond present in endo−exo conformers varies with the electron-donating or -withdrawing strength of each para-substituent. Donors increase electron density around the boron atom and lead to shorter hydrogen bond distances, for example, 2.392 Å for acid **1** (R = OMe). Withdrawing groups do the opposite by drawing electron density away from the boron atom, leading to an increase in oxygen−boron conjugation and a corresponding lengthening of the intramolecular hydrogen bond, for example, 2.407 Å for acid **6** (R = CN). Similar trends can be seen in the variations in the C−B and B−O bond lengths of acids **1**−**6** as well as their O−B−O bond angles (see expanded Table S1 of the Supporting Information). Overall the donating or withdrawing nature of the para-substituent can be observed to influence the structural parameters of boronic acids **1**−**6**. Interestingly, however, no overall trend could be observed relating the nature of the para-substituent and the relative free energies of syn or anti conformations. It is also interesting to note that while the endo−exo and syn conformations are flat, the boronic acid moiety of each anti conformation is observed to twist 25−32° out-of-plane relative to the aryl ring.

Table 3 summarizes the thermochemistry of forming boronate esters **11a**−**f**, diazaboroles **12a**−**f**, oxathiaboroles **13a**−**f**, and dithiaboroles **14a**−**f** via the condensation of boronic acids **1**−**6** with donors **7**−**10**, respectively. Before examining the specific influences of different functional groups, it is worthwhile to note four general trends that emerge from the data presented in Table 3: (i) All but three of the 96 condensation reactions (24 reactions at four levels of theory) are predicted to be endothermic, and in all cases the condensation free energies are predicted to be entropy driven. Furthermore, calculated reaction entropies ($T\Delta S°$) are very similar across nearly all condensation reactions at each level of theory, with MP2 calculations of dithiaboroles **14a**−**f** representing the one exception to this observation. Excluding this one exception, the average $T\Delta S°$ for all reactions is 8.1 kcal/mol with a standard deviation of 0.26 kcal/mol. (ii) The choice of donor significantly impacts the free energy of condensation reactions between donors **7**−**10** and boronic acids **1**−**6**. As a general trend boronate esters **11a**−**f** are predicted to be the most favorable, followed by diazaboroles **12a**−**f**, oxathiaboroles **13a**−**f**, and dithiaboroles **14a**−**f**. This trend is predicted to be almost entirely enthalpy driven as reaction entropies remain relatively constant. Calculations performed at the MP2 level, which predict the energetics of boronate ester and diazaborole formation to be equal within error, represent the one exception to this trend. (iii) In contrast to the choice of donor, the para-substituent of boronic acids **1**−**6** has little impact on calculated reaction free energies. Within each set of condensation products **11**−**14**, the difference between the most and least favored assembly is ≤0.9 kcal/mol at the CBS-QB3 level. (iv) A clear trend exists between the reaction energetics predicted by different levels of theory. For any given condensation reaction MP2 calculations predict the most favorable reaction free energies, followed by CBS-QB3, then B3LYP, and finally M06-2X with successive differences of roughly 2−4 kcal/mol between each different level of theory.

DOI: 10.1021/acs.joc.5b02548
J. Org. Chem. XXXX, XXX, XXX−XXX

Table 2. Intramolecular Hydrogen-Bonding Distances Observed in endo−exo Conformations of Acids 1−6 and Relative Free Energies of syn and anti Conformations[a]

		1	2	3	4	5	6
		(R = OMe)	(R = *t*-Bu)	(R = H)	(R = F)	(R = CO_2Me)	(R = CN)
endo−exo	O−H···O	2.392	2.393	2.393	2.396	2.401	2.407
syn	$\Delta G°$	1.0	1.0	1.3	0.9	0.9	0.7
anti	$\Delta G°$	2.4	2.5	2.6	2.8	2.7	3.0

[a]Distances are given in Å. Free energies are calculated relative to the endo−exo conformation of each boronic acid and are given in kcal/mol. Distances and energies are reported from M06-2X/6-31+G(d,p) calculations.

Table 3. M06-2X, B3LYP, CBS-QB3, and MP2 Calculated Free Energies ($\Delta G°$), Enthalpies ($\Delta H°$), and Entropies ($T\Delta S°$) for Each Condensation Reaction Outlined in Scheme 2[a]

			M06-2X/6-31+G(d,p)			B3LYP/6-311+G(d,p)			CBS-QB3			MP2/aug-cc-pVDZ			exp.
		R =	ΔG	ΔH	$T\Delta S$	ΔG	ΔH	$T\Delta S$	ΔG	ΔH	$T\Delta S$	ΔG	ΔH	$T\Delta S$	ΔG
11	**a**	OMe	−2.1	6.1	8.2	−4.2	3.7	7.9	−6.5	1.2	7.7	−8.2	−0.1	8.1	−2.3
	b	*t*-Bu	−2.0	6.4	8.5	−4.0	4.0	8.0	−6.7	1.3	7.9	−8.1	0.1	8.1	−1.9
	c	H	−1.7	6.5	8.1	−3.8	4.0	7.8	−6.4	1.4	7.8	−7.9	0.2	8.1	−2.5
	d	F	−1.6	6.5	8.1	−3.8	4.1	7.8	−6.5	1.4	7.8	−7.8	0.2	8.0	−2.1
	e	CO_2Me	−1.7	6.8	8.5	−3.5	4.3	7.8	−6.1	1.5	7.6	−7.8	0.3	8.1	−1.4
	f	CN	−1.2	6.9	8.1	−3.4	4.4	7.8	−6.2	1.6	7.8	−7.7	0.4	8.1	−1.1
12	**a**	OMe	2.1	10.3	8.2	−0.6	7.7	8.3	−3.2	5.0	8.2	−8.1	0.2	8.3	3.3
	b	*t*-Bu	1.6	10.2	8.5	−1.9	7.5	9.4	−3.0	4.8	7.9	−8.1	0.0	8.1	2.5
	c	H	1.4	10.0	8.6	−1.1	7.3	8.3	−3.3	4.6	8.0	−8.1	0.0	8.1	3.5
	d	F	1.9	10.1	8.2	−0.9	7.4	8.3	−3.3	4.7	8.0	−7.5	0.1	7.6	3.5
	e	CO_2Me	1.2	9.6	8.5	−1.3	6.8	8.1	−3.3	4.3	7.7	−8.4	−0.3	8.1	2.7
	f	CN	1.4	9.6	8.3	−1.4	6.7	8.1	−3.7	4.2	8.0	−8.4	−0.5	8.0	2.7
13	**a**	OMe	5.2	13.4	8.2	2.7	10.8	8.1	−0.3	7.5	7.8	−5.0	3.1	8.1	[b]
	b	*t*-Bu	5.4	13.8	8.4	2.9	11.0	8.2	−0.6	7.6	8.1	−4.7	3.3	8.0	[b]
	c	H	5.7	13.9	8.2	3.0	11.1	8.1	−0.3	7.7	8.0	−4.6	3.5	8.1	[b]
	d	F	5.7	13.9	8.2	3.1	11.2	8.1	−0.3	7.7	8.0	−4.6	3.5	8.1	[b]
	e	CO_2Me	5.7	14.2	8.5	3.4	11.4	8.0	0.0	7.8	7.8	−4.5	3.5	8.1	[b]
	f	CN	6.2	14.3	8.1	3.4	11.4	8.1	−0.2	7.9	8.0	−4.5	3.6	8.0	[b]
14	**a**	OMe	12.4	18.8	6.4	8.8	16.4	7.6	4.6	11.8	7.2	−4.1	1.5	5.6	[b]
	b	*t*-Bu	12.2	19.7	7.5	9.4	16.6	7.2	3.7	11.7	8.0	−3.7	1.6	5.3	[b]
	c	H	10.4	20.3	9.9	9.5	16.7	7.2	4.6	11.9	7.3	−2.4	1.3	3.7	[b]
	d	F	11.1	19.8	8.8	9.7	16.8	7.1	4.3	11.9	7.7	−4.6	2.0	6.6	[b]
	e	CO_2Me	11.4	20.8	9.3	9.3	16.8	7.5	4.2	11.9	7.7	−3.7	1.9	5.5	[b]
	f	CN	11.4	20.8	9.5	9.6	16.9	7.2	3.8	12.1	8.3	−4.0	2.0	5.9	[b]

[a]All values are given in kcal/mol at 298.15 K and 1.0 atm in a PCM implicit solvent model for $CHCl_3$. [b]No equilibrium product formation by ^{1}H NMR spectroscopy.

Upon comparing experimental results presented in Table 1 with computational results of Table 3, it is clear that computational results at the M06-2X/6-31+G(d,p) level are the most consistent with experimental data. Computations at the M06-2X level predict the equilibrium free energy of forming boronate esters **11a−f** to range from $\Delta G° = -1.2$ to -2.1 kcal/mol. This range is in reasonable agreement with experimental results ($\Delta G°_{exp} = -1.1$ to -2.5 kcal/mol). The average difference between experimental and computational M06-2X results for individual boronate ester condensation reactions is ±0.3 kcal/mol with a maximum difference of ±0.8 kcal/mol (product **11c**). It is also observed that M06-2X results are in the best agreement with experimental free energies of diazaborole formation, though the agreement between experimental and computational results is not as good. The calculated free energies for the formation of diazaboroles **12a−f** range from $\Delta G° = 1.2-2.1$ kcal/mol, while spectroscopic results give condensation free energies between $\Delta G° = 2.5-3.5$ kcal/mol. In the case of diazaborole formation, the average difference between experimental and computational results is 1.5 kcal/mol with a maximum deviation of 2.1 kcal/mol (product **12c**).

B3LYP, CBS-QB3, and MP2 calculations predict reaction free energies for boronate ester and diazaborole formation to be more negative, i.e., more favorable, than ^{1}H NMR spectroscopic results reveal. B3LYP/6-311+G(d,p) calculations, for example, predict reaction free energies between $\Delta G° = -3.4$ to -4.2 kcal/mol for the formation of boronate esters **11a−f**. Given the reaction stoichiometry and concentrations of reactants, such reaction free energies would predict that all six boronate esters would be be formed in 98−99% yield at equilibrium. B3LYP predictions are, therefore, relatively consistent with spectroscopic results for the formation of boronate esters **11a−d** given the detection limits of ^{1}H NMR spectroscopy, however, the agreement is considerably less consistent than calculations performed at the M06-2X level. Calculations performed at the CBS-QB3 and MP2/aug-cc-pVDZ levels suggest that all boronate ester condensation reactions investigated have reaction free energies that are exergonic by at least −6.1 kcal/mol, which would correspond to ≥99.7% formation of

DOI: 10.1021/acs.joc.5b02548
J. Org. Chem. XXXX, XXX, XXX−XXX

boronate esters **11a–f** at equilibrium. This computational prediction is clearly not consistent with ^{1}H NMR spectroscopic results that all show measurable amounts of unassembled starting materials present.

In comparing computational and experimental results for diazaborole condensation reactions, it is again clear that B3LYP, CBS-QB3, and MP2 calculations predict reaction free energies that are too favorable to be within reasonable agreement with spectroscopic results. Formation of diazaboroles **12a–f** from the condensation of *ortho*-phenylenediamine with boronic acids **1–6** is predicted to be exergonic by ΔG° = −0.6 to −1.9 kcal/mol at the B3LYP/6-311+G(d,p) level. If the condensation reactions were that favorable then diazaboroles **12a–f** would be present in 80–92% yield at equilibrium, in clear contrast to results obtained spectroscopically. Again, CBS-QB3 and MP2 calculations predict the condensation reactions to be even more exergonic ($\Delta G^\circ_{\text{CBS-QB3}}$ = −3.0 to −3.7 kcal/mol and $\Delta G^\circ_{\text{MP2}}$ = −7.5 to −8.4 kcal/mol), suggesting >97% diazaborole formation at equilibrium. Lastly, no oxathiaborole (**13a–f**) formation is observed by ^{1}H NMR spectroscopy, yet computational results at the B3LYP, CBS-QB3, and MP2 levels each predict equilibrium formation of oxathiaborole products ranging from 20 to 30% (B3LYP) to >99% (MP2). Computational results obtained at the M06-2X level are again more consistent with experimental results, predicting the formation of oxathiaboroles to be endergonic by 5.2–6.2 kcal/mol, which would correspond to a maximum of <8% oxathiaborole formation at equilibrium. An 8% yield of oxathiaborole species would be detectable by ^{1}H NMR spectroscopy, which suggests the M06-2X results likely overestimate the favorability of oxathiaborole formation, however M06-2X computations are still the most consistent with experimental results.

Electronic and Structural Effects. Both experimental and computational investigations reveal that the choice of donor (**7–10**) plays a primary role in determining the favorability of forming a condensation product with boronic acids **1–6**, while the para-substituent of the boronic acids plays a much more secondary role. Still, the subtle influence of the para-substituent of boronic acids **1–6** can be observed both structurally and electronically when comparing results obtained from computations. For example, a general trend is observed in both experimental and computed free energies of boronate ester condensations wherein electron-donating substituents tend to increase the favorability of forming boronate esters, while electron-withdrawing substituents decrease the favorability of their formation. This trend correlates reasonably well with differences in B–O and C–B bond lengths measured in the optimized structures of boronates **11a–f** as shown in Table 4. Boronate esters with donating substituents are found to exhibit longer B–O bond lengths and shorter C–B bond lengths relative to boronate esters with withdrawing groups, though the differences are very small. This trend likely arises because para donating substituents are able to increase the electron density around the boron atom, therefore shortening and strengthening the C–B bond while at the same time reducing electron donation from the oxygen atoms of the catechol moiety, leading to longer B–O bond lengths. Para withdrawing groups decrease electron density at the boron atom, accounting for the longer C–B bonds and shorter B–O bonds as catechol oxygen atoms donate electron density to the electron-poor boron atom. For all esters **11a–f** the C–O bond lengths fall within the tight range of 1.379–1.381 Å, which is longer than the average C–O bond length in catechol itself (1.369 Å), further supporting the notion that catechol behaves as a donor in the boronate ester condensation reactions. Computed electrostatic potential maps shown in Figure 4 further support these observations.

Table 4. Bond Lengths (Å) of B–O and C–B Bonds in Boronate Esters 11a–f along with Hammett σ Constants for Each para-Substituent

	11a	11b	11c	11d	11e	11f
R	OMe	*t*-Bu	H	F	CO_2Me	CN
σ_p	−0.27	−0.20	0.00	0.06	0.45	0.66
B–O (Å)	1.397	1.396	1.395	1.394	1.392	1.391
C–B (Å)	1.533	1.537	1.539	1.539	1.543	1.545

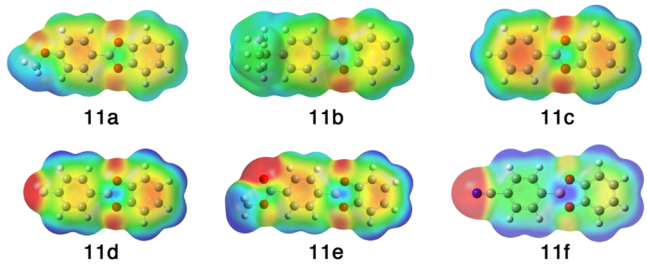

Figure 4. Electron density maps of boronate esters **11a–f** (isovalues: −0.02 to 0.02) calculated at the B3LYP/6-311+G(d,p) level.

Progressing from more donating substituents to more withdrawing substituents results in an easily observable decrease in electron density at the boron atom of esters **11a–f** as well as a decrease in electron density around the periphery of the catechol moiety.

Similar trends in electron density and C–B and B–N bond lengths can be observed for diazaboroles **12a–f** (see Figure S23 and Table S2 of the Supporting Information). Computations predict greater electron density around the boron atom of each diazaborole **12a–f** relative to its corresponding boronate ester analogue **11a–f**. As mentioned earlier, the hydrolytic stability of boronate esters correlates well with the electron density at their boron atom. Diazaboroles are known to be less hydrolytically stable than boronate esters, however their susceptibility to hydrolysis results not from differences in electron density but rather from general differences in the strengths of a typical B–O versus B–N bond. No clear trend could be observed between the nature of the para-substituent of boronic acids **1–6** and the favorability of their condensation with *ortho*-phenylenediamine **8**. Both experimental and computational results suggest that the least favored (most endergonic) diazaborole condensation reactions involve the formation of methoxy-substituted diazaborole **12a** and fluoro-substituted diazaborole **12d**. Interestingly, the most favored (least endergonic) diazaborole condensations are those that form diazaboroles **12e** and **12f** bearing withdrawing methyl ester and cyano functionalities, respectively. When discussing experimental diazaborole results we had postulated that the favorability of forming boroxine anhydride species may account for differences in the equilibrium constants of diazaborole formation, noting that the boroxine of *para*-methoxyphenylboronic acid **1** is more thermodynamically stable[17] than that of *para*-cyanophenylboronic acid **6**. Computational results suggest that boroxine formation may not be the only influence, as

DOI: 10.1021/acs.joc.5b02548
J. Org. Chem. XXXX, XXX, XXX–XXX

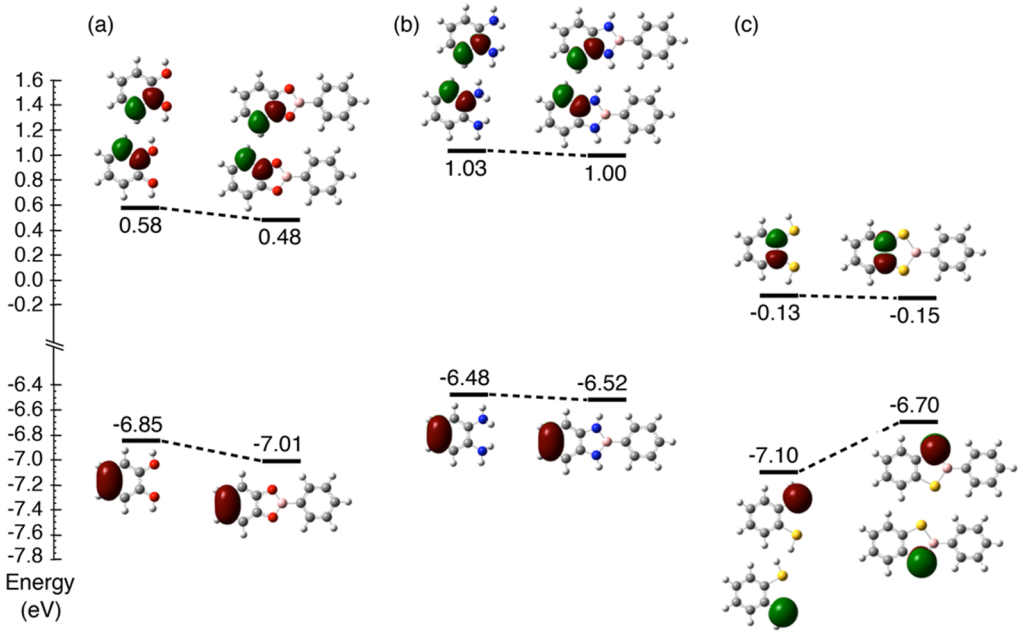

Figure 5. Energies (eV, B3LYP/6-311+G(d,p)) and electron density maps of the HOMOs and LUMOs of (a) catechol, (b) *ortho*-phenylenediamine, and (c) benzene-1,2-dithiol along with the corresponding molecular orbitals upon condensation with phenylboronic acid.

calculations at the M06-2X/6-31+G(d,p) level are in line with the experimental observation that the formation of cyano-substituted diazaborole **12f** is more favored than methoxy-substituted diazaborole **12a** even though computational results do not take boroxine formation into account. It should be stressed, however, that both computationally predicted and experimentally observed differences between the condensation free energies of diazaboroles **12a–f** are so similar that they are within error, and it is likely not possible to definitively determine what accounts for the small differences between condensation free energies.

Significantly greater differences are observed when comparing condensation reactions involving different donors, i.e., **7**–**10**. To better understand these differences in reactivity, we investigated the effects of borylation on catechol, *ortho*-phenylenediamine, and benzene-1,2-dithiol, which serve as model systems of *tert*-butylcatechol (**7**), *tert*-butyl-*ortho*-phenylenediamine (**8**), and toluene-3,4-dithiol (**10**). More specifically, natural bond order[49] calculations were carried out to examine the influence of borylation on the frontier orbitals of the three different classes of donors. Figure 5 shows the HOMO and LUMO orbitals of catechol (Figure 5a), *ortho*-phenylenediamine (Figure 5b), and benzene-1,2-dithiol (Figure 5c) along with the corresponding orbitals of their boronate ester, diazaborole, and dithiaborol products formed upon condensation with phenylboronic acid **3**. Catechol and *ortho*-phenylenediamine each have a nondegenerate HOMO that corresponds to the π bond between the 4 and 5 carbons (C_4–C_5) of their respective aromatic rings. The LUMO orbitals of catechol and *ortho*-phenylenediamine are both doubly degenerate and correspond to π^* antibonding orbitals between C_2–C_3 and C_6–C_1. Condensation of catechol or *ortho*-phenylenediamine with phenylboronic acid results in the stabilization both of these sets of frontier orbitals. For example, the HOMO of catechol (Figure 5a) is lowered by 0.16 eV upon condensation to the corresponding boronate ester, while the LUMO is 0.10 eV more stable. Borylation of *ortho*-phenylenediamine to give the corresponding diazaborole also results in a stabilization of the *ortho*-phenylenediamine HOMO and LUMO orbitals, though to a lesser extent (0.04 and 0.03 eV, respectively) as shown in Figure 5b.

The frontier orbitals and effects of borylation are notably different in the case of benzene-1,2-dithiol as compared to catechol and *ortho*-phenylenediamine. The HOMO of benzene-1,2-dithiol is doubly degenerate and corresponds to the lone pair P_z orbital of each of the two sulfur atoms (Figure 5c). The LUMO is nondegenerate and corresponds to the C_1–C_2 antibonding π^* orbital. Borylation of benzene-1,2-dithiol to give the corresponding dithiaborole results in a 0.02 eV stabilization of the C_1–C_2 π^* antibonding orbital but a 0.40 eV destabilization of the degenerate lone pair P_z orbitals of the sulfur atoms. This destabilization mirrors the overall trend observed throughout this study, namely that boronate ester formation is somewhat more thermodynamically favorable than diazaborole formation, while both boronate and diazaborole formations are notably more favorable than dithiaborole formation. This general trend can again be observed when comparing the lengths of B–X bonds (where X = O, NH, or S), wherein stronger bonds are typically shorter than the sum of the covalent radii of their constituent atoms. Indeed B–O and B–N(H) bond lengths obtained from calculations (Table 5) are both 7% shorter than the sum of the covalent radii[50] of their constituent atoms. The calculated length of the B–S bond, by contrast, is only 4% shorter than the sum of boron and sulfur covalent radii. This observation further supports the conclusion that B–S bonds of dithiaboroles are weaker than the B–O and B–(NH) bonds of boronate esters and diazaboroles, respectively. Collectively the computationally observed differences in bond lengths and the effects of borylation on the frontier molecular orbitals of catechol, *ortho*-phenylenediamine, and benzene-1,2-dithiol help rationalize the large differences between reaction enthalpies ($\Delta H°$, Table 3) for the formation of aryl boronate ester, diazaborole, and dithiaborole condensation products.

DOI: 10.1021/acs.joc.5b02548
J. Org. Chem. XXXX, XXX, XXX–XXX

Table 5. Predicted and Calculated Bond Lengths[a] of B−O, B−(NH), and B−S Bonds in Boronate Ester 11c, Diazaborole 12c, and Dithiaborole 14c

bond	predicted (Å)	calculated (Å)	difference
B−O	1.50	1.39	0.11 (7.3%)
B−(NH)	1.55	1.44	0.11 (7.1%)
B−S	1.89	1.81	0.08 (4.2%)

[a]Bond lengths are predicted from covalent radii of boron (0.84 Å), oxygen (0.66 Å), nitrogen (0.71 Å), and sulfur (1.05 Å).[50] Computed bond lengths are reported at the M06-2X/6-31+G(d,p) level, however they are identical to within 3 significant figures to bond lengths computed using DFT and CBS-QB3. MP2 calculated bond lengths were each 0.01 Å longer.

CONCLUSIONS

The results presented herein provide a greater understanding of the energetics of dynamic covalent condensation reactions between para-substituted arylboronic acids with diol, diamine, mercaptophenol, and dithiol donors to give boronate esters, diazaboroles, oxathiaboroles, and dithiaboroles, respectively. Both experimental and computational results show that the electron-donating or -withdrawing nature of the para-substituent of the arylboronic acid plays a relatively small role in influencing the favorability of forming a condensation product with any of the donors. The choice of donor, on the other hand, significantly influences the favorability of forming a condensation product. Only two of the four classes of donors undergo spontaneous self-assembly with the para-substituted arylboronic acids investigated: 4-*tert*-butylcatechol (**7**) and 4-*tert*-butyl-*ortho*-phenylenediamine (**8**). Catechol **7** readily assembles with the arylboronic acids to give boronate ester products in high yields (>90%) at equilibrium. The assembly of diazaboroles from condensation of the *ortho*-phenylenediamine **8** and aylboronic acids is less favorable thermodynamically, giving diazaborole products in more moderate yields (30−44%) at equilibrium. Neither of the remaining two donors, 2-hydroxybenzenethiol (**9**) and toluene-3,4-dithiol (**10**), could be observed to undergo dynamic covalent self-assembly with any of the arylboronic acids in chloroform at room temperature. Computational results carried out at four different levels of theory generally support the experimental observations that para-substituents have little influence on the energetics of self-assembly, while the donor has a large influence. While the different computational methods agree on these overall trends, they differ significantly in their predictions of reaction free energies and reaction enthalpies for boronate ester, diazaborole, oxathiaborole, and dithiaborole formation. Calculations carried out at the M06-2X /6-31+G(d,p) level were found to be the most consistent with experimental results, while B3LYP, CBS-QB3, and MP2 calculations each predicted reaction energetics that were notably more favorable than those found experimentally. Given the increasing use of boronic acids in the dynamic covalent self-assembly of polymers, COFs, and other organic materials, it is important to understand how different functionalities influence the favorability of assembly formation. This study of the self-assembly of boronate esters, diazaboroles, oxathiaboroles, and dithiaboroles in an organic solvent helps provide that understanding, allows for direct comparisons across different classes of donors and/or arylboronic acids, and gives insight into which computational methods are most appropriate for modeling these important classes of compounds.

COMPUTATIONAL AND EXPERIMENTAL METHODS

Computational Details. All calculations were performed with the Gaussian09 suite of programs.[51] Initial structures were built within the GaussView interface and then conformationally searched by scanning all easily rotating dihedral angles at the HF/6-31G(g) level of theory. Approximate global energy minima obtained from conformational searches were then optimized to full convergence and subjected to vibrational and thermal analysis at each of four levels of theory: B3LYP/6-311+G(d,p), M06-2X/6-31+G(d,p), CBS-QB3, and MP2/aug-cc-pVDZ. Geometry optimizations and frequency analysis were performed in an implicit solvent model for chloroform (ε = 4.7113) using the PCM reaction field model.[52] Stationary points were confirmed as minima by the lack of any imaginary vibrational frequencies. All reaction enthalpies ($\Delta H°$), entropies ($\Delta S°$), and free energies ($\Delta G°$) reported in this manuscript were calculated at 1.0 atm pressure, 298.15 K, and in a solvent model for chloroform.

Materials. Chemicals and reagent-grade solvents were obtained from commercial sources and used as purchased. Deuterated chloroform was obtained from Cambridge Isotope Laboratories and dried by passing a freshly opened bottle of $CDCl_3$ over a glass column packed with a small pad of anhydrous Na_2SO_4 on top of basic Al_2O_3 using a positive pressure of dry N_2 gas. The resulting anhydrous $CDCl_3$ was collected in a flame-dried Schlenk flask containing 4 Å molecular sieves and stored under nitrogen.

General Procedure for the Synthesis of Boronate Esters 11a−f. Analytical samples of boronate ester compounds **11a−f** were prepared for spectroscopic comparison with equilibrated mixtures described in Scheme 2. Into a small round-bottom flask were added 200 mg (1.2 mmol) of *tert*-butyl catechol (**7**) and 1.0 molar equiv of a given boronic acid (**1**−**6**). The solids were taken up in 12.0 mL of $CHCl_3$ and stirred at 50 °C for 3 h in the presence of a catalytic amount of DOWEX. The resulting solution was cooled down to room temperature, dried over anhydrous $MgSO_4$, filtered, and concentrated under reduced pressure. The resulting solids were washed with hexanes and ether and then dried under high vacuum to afford pure samples of esters **11a−f**.

***11a**. Reaction Scale.* **7** (200 mg, 1.2 mmol) and **1** (184 mg, 1.2 mmol), yield 295 mg (87%). The product was isolated as white solid. Mp = 123−126 °C. TOF MS CI$^+$ (m/z) $[MH]^+$ calcd for $C_{17}H_{20}{}^{11}BO_3$, 283.1506; found 283.1516. ^{1}H NMR (300 MHz, $CDCl_3$, 298 K) δ = 8.05 (2H, d, J = 8.7 Hz), 7.38 (1H, d, J = 1.8 Hz), 7.22 (1H, d, J = 8.1 Hz), 7.15 (1H, dd, J = 8.1, 1.8 Hz), 7.03 (2H, d, J = 8.7 Hz), 3.88 (3H, s), 1.39 (9H, s). ^{13}C NMR (125 MHz, $CDCl_3$) δ = 163.0, 148.5, 146.4, 146.3, 136.8, 119.3, 113.9, 111.4, 109.8, 55.2, 34.8, 31.8.

***11b**. Reaction Scale.* **7** (200 mg, 1.2 mmol) and **2** (213 mg, 1.2 mmol), yield 336 mg (91%). The product was isolated as white solid. Mp = 97−100 °C. TOF MS CI$^+$ (m/z) $[MH]^+$ calcd for $C_{20}H_{26}{}^{11}BO_2$, 309.2026; found 309.2030. ^{1}H NMR (300 MHz, $CDCl_3$, 298 K) δ = 8.09 (2H, d, J = 8.4 Hz), 7.57 (2H, d, J = 8.4 Hz), 7.43 (1H, d, J = 1.2 Hz), 7.27 (1H, d, J = 8.1 Hz), 7.19 (1H, dd, J = 8.1, 1.2 Hz), 1.42 (18H, s). ^{13}C NMR (125 MHz, $CDCl_3$) δ = 155.7, 148.5, 146.5, 146.4, 135.0, 126.3, 119.4, 111.5, 109.9, 35.1, 34.9, 31.8, 31.2.

***11c**. Reaction Scale.* **7** (200 mg, 1.2 mmol) and **3** (148 mg, 1.2 mmol), yield 240 mg (79%). The product was isolated as white solid. Mp = 49−50 °C. TOF MS EI$^+$ (m/z) $[M]^+$ calcd for $C_{16}H_{17}{}^{11}BO_2$, 252.13217; found 252.13228. ^{1}H NMR (300 MHz, $CDCl_3$, 298 K) δ = 8.15 (2H, d, J = 8.1 Hz), 7.62−7.50 (3H, m), 7.43 (1H, d, J = 1.5 Hz), 7.27 (1H, d, J = 8.7 Hz), 7.20 (1H, dd, J = 8.7, 1.5 Hz), 1.43 (9H, s). ^{13}C NMR (125 MHz, $CDCl_3$) δ = 148.5, 146.6, 146.3, 135.0, 132.3, 128.3, 119.5, 111.6, 110.0, 34.9, 31.9.

***11d**. Reaction Scale.* **7** (200 mg, 1.2 mmol) and **4** (171 mg, 1.2 mmol), yield 276 mg (85%). The product was isolated as white solid. Mp = 106−107 °C. TOF MS EI$^+$ (m/z) $[M]^+$ calcd for $C_{16}H_{16}{}^{11}BO_2F$, 270.12274; found 270.12250. ^{1}H NMR (300 MHz, $CDCl_3$, 298 K) δ = 8.08 (2H, t, J = 6.3 Hz), 7.36 (1H, d, J = 1.2 Hz), 7.26−7.15 (4H, m), 1.37 (9H, s). ^{13}C NMR (125 MHz, $CDCl_3$) δ = 166.7, 164.7, 148.4, 146.5, 138.0, 137.2, 119.5, 115.4, 111.5, 109.8, 34.8, 31.7.

DOI: 10.1021/acs.joc.5b02548
J. Org. Chem. XXXX, XXX, XXX−XXX

11e. Reaction Scale. **7** (200 mg, 1.2 mmol) and **5** (217 mg, 1.2 mmol), yield 340 mg (91%). The product was isolated as white solid. Mp = 155−157 °C. TOF MS CI$^+$ (m/z) [MH]$^+$ calcd for $C_{18}H_{20}{}^{11}BO_4$, 311.1455; found 311.1454. ^{1}H NMR (300 MHz, $CDCl_3$, 298 K) δ = 8.14 (4H, s), 7.38, (1H, d, J = 1.8 Hz), 7.23 (1H, d, J = 8.1 Hz), 7.17 (1H, dd, J = 8.1 Hz, 1.8 Hz), 3.95 (3H, s), 1.36 (9H, s). ^{13}C NMR (125 MHz, $CDCl_3$) δ = 166.8, 148.4, 146.9, 146.1, 134.8, 133.4, 129.0, 119.7, 111.6, 110.0, 52.1, 34.8, 31.7.

11f. Reaction Scale. **7** (200 mg, 1.2 mmol) and **6** (177 mg, 1.2 mmol), yield 273 mg (82%). The product was isolated as white solid. Mp = 174−176 °C. TOF MS EI$^+$ (m/z) [M]$^+$ calcd for $C_{17}H_{16}{}^{11}BO_2N$, 277.12741; found 277.12761. ^{1}H NMR (300 MHz, $CDCl_3$, 298 K) δ = 8.16 (2H, d, J = 8.4 Hz), 7.76 (2H, d, J = 8.4 Hz), 7.39 (1H, d, J = 1.2 Hz), 7.22 (1H, d, J = 8.1 Hz), 7.20 (1H, dd, J = 8.1, 1.2 Hz), 1.36 (9H, s). ^{13}C NMR (125 MHz, $CDCl_3$) δ = 148.2, 147.3, 146.0, 135.2, 131.6, 1120.0, 118.4, 115.7, 111.8, 110.1, 34.9, 31.7.

General Procedure for the Synthesis of Diazaboroles 12a−f. Analytical samples of diazaboroles **12a−f** were prepared by suspending 150 mg (0.91 mmol) of 4-*tert*-butyl-*ortho*-phenylenediamine (**8**) and 1.0 molar equiv of a given boronic acid (**1−6**) in 9.1 mL of toluene in the presence of 4 Å molecular sieves. The mixtures were stirred at 80 °C for 8 h and then filtered hot, washing with hot (∼80 °C) toluene. Diazaboroles **12a**, **12b**, and **12e** (R = OMe, *t*-Bu, and CO_2Me, respectively) crystallized directly from their toluene solutions upon cooling, and the resulting crystals were washed with hexanes and dried under vacuum to give pure diazaborole products. Additional quantities of diazaboroles **12b** and **12e** could be obtained upon concentrating the toluene filtrate. Diazaboroles **12c** and **12d** (R = F and Ph, respectively) were isolated by concentrating their toluene filtrates and recrystallizing from warm hexanes. Lastly, diazaborole **12f** (R = CN) required additional heating (refluxing toluene, Dean−Stark apparatus, 18 h) followed by drying the resulting solution over $MgSO_4$, filtering, concentrating under reduced pressure, and washing with cold hexanes.

12a. Reaction Scale. **8** (150 mg, 0.91 mmol) and **1** (138 mg, 0.91 mmol), yield 242 mg (95%). The product was isolated as needle-like white solid crystals. Mp = 253−255 °C. TOF MS EI$^+$ (m/z) [M]$^+$ calcd for $C_{17}H_{21}{}^{11}BON_2$, 280.17471; found 280.17469. ^{1}H NMR (300 MHz, $CDCl_3$, 298 K) δ = 7.66 (2H, d, J = 8.4 Hz), 7.15 (1H, s), 7.01−6.96 (4H, m), 6.63 (2H, br, −N*H*−), 3.86 (3H, s), 1.36 (9H, s). ^{13}C NMR (125 MHz, $CDCl_3$, poor solubility limited signal-to-noise of quaternary carbon signals) δ = 134.5, 116.2, 113.9, 110.2, 108.2, 55.1, 32.0.

12b. Reaction Scale. **8** (150 mg, 0.91 mmol) and **2** (163 mg, 0.91 mmol), yield 245 mg (88%). The product was isolated as white crystalline solid. Mp = 213−215 °C. TOF MS EI$^+$ (m/z) [M]$^+$ calcd for $C_{20}H_{27}{}^{11}BN_2$, 306.22674; found 306.22709. ^{1}H NMR (300 MHz, $CDCl_3$, 298 K) δ = 7.72 (2H, d, J = 8.1 Hz), 7.51 (2H, d, J = 8.1 Hz), 7.21 (1H, s), 7.10−7.04 (4H, m), 6.74−6.71 (2H, br, −N*H*−), 1.41−1.40 (18H, s). ^{13}C NMR (125 MHz, $CDCl_3$) δ = 152.8, 142.8, 136.3, 134.2, 132.9, 125.2, 116.4, 110.4, 108.3, 34.8, 34.5, 32.0, 31.3.

12c. Reaction Scale. **8** (150 mg, 0.91 mmol) and **3** (111 mg, 0.91 mmol), yield 191 mg (84%). The product was isolated as a white solid. Mp = 191−192 °C. TOF MS EI$^+$ (m/z) [M]$^+$ calcd for $C_{16}H_{19}{}^{11}BN_2$, 250.16414; found 250.16439. ^{1}H NMR (300 MHz, $CDCl_3$, 298 K) δ = 7.77 (2H, dd, J = 9.3, 3.3 Hz), 7.49−7.46 (3H, m), 7.22 (1H, s), 7.10−7.07 (2H, m), 6.73 (2H, br, −N*H*−), 1.42 (9H, s). ^{13}C NMR (125 MHz, $CDCl_3$) δ = 152.8, 142.8, 136.3, 134.2, 132.9, 125.2, 116.4, 110.4, 108.3, 34.8, 34.5, 32.0, 31.3.

12d. Reaction Scale. **8** (150 mg, 0.91 mmol) and **4** (127 mg, 0.91 mmol), yield 214 mg (88%). The product was isolated as white solid flakes. Mp = 186−187 °C. TOF MS EI$^+$ (m/z) [M]$^+$ calcd for $C_{16}H_{18}{}^{11}BN_2F$, 268.15471; found 268.15459. ^{1}H NMR (300 MHz, $CDCl_3$, 298 K) δ = 7.71 (2H, t, J = 6.3 Hz), 7.20 (1H, s), 7.14 (2H, t, J = 6.3 Hz), 7.08−7.05 (2H, m), 6.67 (2H, br, −N*H*−), 1.40 (9H, s). ^{13}C NMR (125 MHz, $CDCl_3$) δ = 165.1, 163.1, 143.0, 136.2, 134.8, 134.0, 116.6, 115.2, 110.5, 108.4, 34.5, 31.9.

12e. Reaction Scale. **8** (150 mg, 0.91 mmol) and **5** (164 mg, 0.91 mmol), yield 230 mg (82%). The product was isolated as a white solid. Mp = 212−213 °C. TOF MS EI$^+$ (m/z) [M]$^+$ calcd for $C_{18}H_{21}{}^{11}BO_2N_2$, 308.16962; found 308.16974. ^{1}H NMR (300 MHz, $CDCl_3$, 298 K) δ = 8.14 (4H, br), 7.38 (1H, d, J = 1.8 Hz), 7.23 (1H, d, J = 8.1 Hz), 7.17 (1H, dd, J = 8.1, 1.8 Hz), 3.95 (3H, s), 1.36 (9H, s). ^{13}C NMR (125 MHz, $CDCl_3$) δ = 167.2, 143.2, 136.1, 133.9, 133.0, 130.9, 129.1, 116.8, 110.7, 108.6, 52.2, 34.5, 32.0.

12f. Reaction Scale. **8** (150 mg, 0.91 mmol) and **6** (134 mg, 0.91 mmol), yield 168 mg (67%). The product was isolated as a light-brown oil that gradually solidifies upon sitting. Mp = 65−69 °C. TOF MS EI$^+$ (m/z) [M]$^+$ calcd for $C_{17}H_{18}{}^{11}BN_3$, 275.15938; found 275.15974. ^{1}H NMR (300 MHz, $CDCl_3$, 298 K) δ = 7.79 (2H, d, J = 8.4 Hz), 7.69 (2H, d, J = 8.4 Hz), 7.21 (1H, s), 7.08−7.06 (2H, m), 6.82 (2H, br, −N*H*−), 1.37 (9H, s). ^{13}C NMR (125 MHz, $CDCl_3$) δ = 143.6, 136.2, 134.0, 133.5, 131.6, 125.5, 119.2, 117.2, 112.8, 111.0, 108.9, 34.6, 32.1.

General Procedure for the Equilibration of Boronate Esters 11a−f and Diazaboroles 12a−f. When setting up equilibration reactions involving boronic acids, it is important to ensure that water moisture is excluded from starting materials, glassware, and solvents so that excess water does not unduly influence the resulting equilibrium. Therefore, all NMR tubes, round-bottom flasks, and glass vials used were oven-dried overnight at >115 °C. A freshly opened bottle of $CDCl_3$ was dried as described in the above Materials section. Stock solutions of 4-*tert*-butylcatechol (**7**) and 4-*tert*-butyl-*ortho*-phenylenediamine (**8**) were prepared by weighing out 108 mg of **7** and 106.8 mg of **8** (6.5×10^{-4} mol in each case) into separate 25 mL round-bottom flasks. The flasks were then capped with a rubber septum, placed under vacuum, briefly flame-dried to further remove trace moisture, and placed under dry $N_{2(g)}$. Once cooled down to room temperature, 13 mL of dry $CDCl_3$ was added to each sample of **7** and **8** via syringe, resulting in 0.05 M stock solutions of each donor. Into separate 2 dram vials were weighed 0.05 mmol of each boronic acid **1−6**. Each vial was capped with a septum and placed under vacuum for 10 min (Note: placing the boronic acids under vacuum for longer periods of time, oven drying, or exposing them to flame drying, results in significant to quantitative formation of their boroxine anhydrides. This should be avoided as it changes the nature, and therefore energetics, of the dynamic covalent reactions leading to **11a−f** and **12a−f** because the starting materials are no longer boronic acids **1−6**). A 1.0 mL sample of the stock solution of **7** or **8** was added to each boronic acid vial giving a 1:1 molar ratio of donor and boronic acid (0.05 M). Each mixture was briefly agitated, transferred to an oven-dried NMR tube via syringe, and capped, and the caps were wraped with Teflon tape. ^{1}H NMR spectra were periodically taken of each mixture until no changes in spectral signals or their integration could be observed, indicating that equilibrium had been reached.

■ ASSOCIATED CONTENT

Supporting Information

The Supporting Information is available free of charge on the ACS Publications website at DOI: 10.1021/acs.joc.5b02548.

^{1}H and ^{13}C NMR spectra of boronate esters **11a−f** and diazaboroles **12a−f**, ^{1}H NMR spectra of boronic acids **1−6** and their boroxine anhydrides, ^{1}H NMR spectra of equilibrated mixtures of all boronate ester and diazaborole assemblies, expanded tables detailing the relative energetics, bond lengths, and bond angles of different boronic acid conformations, tables of calculated bond distances of diazaboroles **12a−f**, oxathiaboroles **13a−f**, and dithiaboroles **14a−f**, calculated electron density maps of diazaborole and dithiaborole species, Cartesian coordinates of all stationary points reported in this manuscript and their absolute free energies in hartrees, and complete ref 51 (PDF)

■ AUTHOR INFORMATION

Corresponding Author

*E-mail: bnorthrop@wesleyan.edu.

DOI: 10.1021/acs.joc.5b02548
J. Org. Chem. XXXX, XXX, XXX−XXX

Notes

The authors declare no competing financial interest.

■ ACKNOWLEDGMENTS

This research was supported by Wesleyan University. We thank Wesleyan University for computer time supported by the NSF under grant number CNS-0619508.

■ REFERENCES

(1) (a) Wu, X.; Li, Z.; Chen, X. X.; Fossey, J. S.; James, T. D.; Jiang, Y. B. *Chem. Soc. Rev.* **2013**, *42*, 8032−8048. (b) Whyte, G. F.; Vilar, R.; Woscholski, R. *J. Chem. Biol.* **2013**, *6*, 161−174. (c) Bull, S. D.; Davidson, M. G.; Vanden Elsen, J. M. H.; Fossey, J. S.; Jenkins, A. T. A.; Jiang, Y. B.; Kubo, Y.; Marken, F.; Sakurai, K.; Zhao, J. Z.; James, T. D. *Acc. Chem. Res.* **2013**, *46*, 312−326. (d) Mader, H. S.; Wolfbeis, O. S. *Microchim. Acta* **2008**, *162*, 1−34. (e) Cao, H. S.; Heagy, M. D. *J. Fluoresc.* **2004**, *14*, 569−584. (f) Wang, W.; Gao, X. M.; Wang, B. H. *Curr. Org. Chem.* **2002**, *6*, 1285−1317.

(2) (a) Martinez-Aguirre, M. A.; Yatsimirsky, A. K. *J. Org. Chem.* **2015**, *80*, 4985−4993. (b) Zhou, Y.; Zhang, J.; Yoon, J. *Chem. Rev.* **2014**, *114*, 5511−5571. (c) Wade, C. R.; Broomsgrove, A. E. J.; Aldridge, S.; Gabbai, F. P. *Chem. Rev.* **2010**, *110*, 3958−3984.

(3) (a) Ito, S.; Ono, K.; Iwasawa, N. *J. Am. Chem. Soc.* **2012**, *134*, 13962−13965. (b) Christinat, N.; Scopelliti, R.; Severin, K. *Angew. Chem.* **2008**, *120*, 1874−1878. (c) Iwasawa, N.; Takahagi, H. *J. Am. Chem. Soc.* **2007**, *129*, 7754−7755.

(4) (a) Nishimura, N.; Kobayashi, K. *J. Org. Chem.* **2010**, *75*, 6079−6085. (b) Nishimura, N.; Yoza, K.; Kobayashi, K. *J. Am. Chem. Soc.* **2010**, *132*, 777−790. (c) Icli, B.; Christinat, N.; Tönnemann, J.; Schüttler, C.; Scopelliti, R.; Severin, K. *J. Am. Chem. Soc.* **2009**, *131*, 3154−3155. (d) Takahagi, H.; Fujibe, S.; Iwasawa, N. *Chem. - Eur. J.* **2009**, *15*, 13327−13330. (e) Nishimura, N.; Kobayashi, K. *Angew. Chem., Int. Ed.* **2008**, *47*, 6255−6258. (f) Kataoka, K.; James, T. D.; Kubo, Y. *J. Am. Chem. Soc.* **2007**, *129*, 15126−15127.

(5) See, for example: (a) Cromwell, O. R.; Chung, J.; Guan, Z. *J. Am. Chem. Soc.* **2015**, *137*, 6492−6495. (b) Cai, M.; Daniel, S. L.; Lavigne, J. J. *Chem. Commun.* **2013**, *49*, 6504−6506. (c) Roy, D.; Cambre, J. N.; Sumerlin, B. S. *Chem. Commun.* **2009**, 2106−2108. (d) Sanchez, J. C.; Trogler, W. C. *J. Mater. Chem.* **2008**, *18*, 5134−5141. (e) Christinat, N.; Croisier, E.; Scopelliti, R.; Cascella, M.; Röthlisberger, U.; Severin, K. *Eur. J. Inorg. Chem.* **2007**, *2007*, 5177−5181. (f) Niu, W.; Smith, M. D.; Lavigne, J. J. *J. Am. Chem. Soc.* **2006**, *128*, 16466−16467. (g) Niu, W.; O'Sullivan, C.; Rambo, B. M.; Smith, M. D.; Lavigne, J. J. *Chem. Commun.* **2005**, 4342−4344. (h) Nakazawa, I.; Suda, S.; Masuda, M.; Asai, M.; Shimizu, T. *Chem. Commun.* **2000**, 881−882. (i) Mikami, M.; Shinkai, S. *Chem. Lett.* **1995**, *24*, 603−604.

(6) For recent reviews of COFs see: (a) Xiang, Z.; Cao, D.; Dai, L. *Polym. Chem.* **2015**, *6*, 1896−1911. (b) Colson, J. W.; Dichtel, W. R. *Nat. Chem.* **2013**, *5*, 453−465. (c) Ding, S.-Y.; Wang, W. *Chem. Soc. Rev.* **2013**, *42*, 548−568. (d) Feng, X.; Ding, X.; Jiang, D. *Chem. Soc. Rev.* **2012**, *41*, 6010−6022. (e) Furukawa, H.; Yaghi, O. M. *J. Am. Chem. Soc.* **2009**, *131*, 8875−8883.

(7) Hall, D. G. *Boronic Acids*, 1st ed; Wiley-VCH: Weinheim, 2006; pp 1−26.

(8) Severin, K. *Dalton Trans.* **2009**, 5254−5264.

(9) Fujita, N.; Shinkai, S.; James, T. D. *Chem. - Asian J.* **2008**, *3*, 1076−1091.

(10) Korich, A. L.; Iovine, P. M. *Dalton Trans.* **2010**, *39*, 1423−1431.

(11) Tokunaga, Y. *Heterocycles* **2013**, *87*, 991−1021.

(12) Lorand, J. P.; Edwards, J. O. *J. Org. Chem.* **1959**, *24*, 769−774.

(13) Springsteen, G.; Wang, B. *Tetrahedron* **2002**, *58*, 5291−5300.

(14) Arzt, M.; Seidler, C.; Ng, D. Y. W.; Weil, T. *Chem. - Asian J.* **2014**, *9*, 1994−2003.

(15) Marinaro, W. A.; Prankerd, R.; Kinnari, K.; Stella, V. J. *J. Pharm. Sci.* **2015**, *104*, 1399−1408.

(16) Dichtel et al. have investigated dynamic exchange processes between different boronate esters and boronic acids as part of a mechanistic investigation of COF formation, see: Spitler, E. L.; Giovino, M. R.; White, S. L.; Dichtel, W. R. *Chem. Sci.* **2011**, *2*, 1588−1593.

(17) Tokunaga, Y.; Ueno, H.; Shimomura, Y.; Seo, T. *Heterocycles* **2002**, *57*, 787−790.

(18) Tokunaga, Y.; Ueno, H.; Shimomura, Y. *Heterocycles* **2007**, *74*, 219−223.

(19) Kua, J.; Iovine, P. *J. Phys. Chem. A* **2005**, *109*, 8938−8943.

(20) Fielder, W. L.; Chamberlain, M. M.; Brown, C. A. *J. Org. Chem.* **1961**, *26*, 2154−2155.

(21) (a) Das, M. K.; Mariategui, J. F.; Niedenzu, K. *Inorg. Chem.* **1987**, *26*, 3114−3116. (b) Mariategui, J. F.; Niedenzu, K. *J. Organomet. Chem.* **1989**, *369*, 137−145.

(22) Beckett, M. A.; Strickland, G. C.; Varma, K. S.; Hibbs, D. E.; Hursthouse, M. B.; Malik, K. M. A. *J. Organomet. Chem.* **1997**, *535*, 33−41.

(23) Perttu, E. K.; Arnold, M.; Iovine, P. M. *Tetrahedron Lett.* **2005**, *46*, 8753−8756.

(24) (a) Kua, J.; Gyselbrecht, C. R. *J. Phys. Chem. A* **2008**, *112*, 9128−9133. (b) Iovine, P. M.; Gyselbrecht, C. R.; Perttu, E. K.; Klick, C.; Neuwelt, A.; Loera, J.; DiPasquale, A. G.; Rheingold, A. L.; Kua, J. *Dalton Trans.* **2008**, 3791−3794. (c) Kua, J.; Gyselbrecht, C. R. *J. Phys. Chem. A* **2007**, *111*, 4759−4776. (d) Kua, J.; Fletcher, M. N.; Iovine, P. M. *J. Phys. Chem. A* **2006**, *110*, 8158−8166.

(25) Substituted diazaboroles have more commonly been prepared by reacting 2-bromo-1,3-di(alkyl)-1,3,2-diazaboroles with alkyl or aryl lithium compounds than by boronic acid-diamine condensation reactions (see, e.g.: Weber, L.; Eickhoff, D.; Werner, V.; Böhling, L.; Schwedler, S.; Chrostowska, A.; Dargelos, A.; Maciejczyk, M.; Stammler, H.-G.; Neumann, B. *Dalton Trans.* **2011**, *40*, 4434−4446.

(26) Letsinger, R. L.; Hamilton, S. B. *J. Am. Chem. Soc.* **1958**, *80*, 5411−5413.

(27) Maruyama, S.; Kawanishi, Y. *J. Mater. Chem.* **2002**, *12*, 2245−2249.

(28) Yamaguchi, I.; Choi, B.-J.; Koizumi, T.-a.; Kubota, K.; Yamamoto, T. *Macromolecules* **2007**, *40*, 438−443.

(29) Kojima, T.; Kumaki, D.; Nishida, J.-I.; Tokito, S.; Yamashita, Y. *J. Mater. Chem.* **2011**, *21*, 6607−6613.

(30) (a) Yamashita, M.; Yamamoto, Y.; Akiba, K.-Y.; Nagase, S. *Angew. Chem., Int. Ed.* **2000**, *39*, 4055−4058. (b) Yamashita, M.; Yamamoto, Y.; Akiba, K.-Y.; Hashizume, D.; Iwasaki, F.; Takagi, N.; Nagase, S. *J. Am. Chem. Soc.* **2005**, *127*, 4354−4371.

(31) Goswami, A.; Maier, C.-J.; Pritzkow, H.; Siebert, W. *Eur. J. Inorg. Chem.* **2004**, *2004*, 2635−2645.

(32) Solomon, S. A.; Del Grosso, A.; Clark, E. R.; Bagutski, V.; McDouall, J. J. W.; Ingleson, M. J. *Organometallics* **2012**, *31*, 1908−1916.

(33) For reviews of dynamic covalent self-assembly see: (a) Jin, Y.; Wang, Q.; Taynton, P.; Zhang, W. *Acc. Chem. Res.* **2014**, *47*, 1575−1586. (b) Corbett, P. T.; LeClaire, J.; Vial, L.; West, K. R.; Wietor, J.-L.; Sanders, J. M. K.; Otto, S. *Chem. Rev.* **2006**, *106*, 3652−3711. (c) Rowan, S. J.; Cantrill, S. J.; Cousins, G. R. L.; Sanders, J. K. M.; Stoddart, J. F. *Angew. Chem., Int. Ed.* **2002**, *41*, 898−952.

(34) Cabiddu, S.; Maccioni, A.; Mura, L.; Secci, M. *J. Heterocycl. Chem.* **1975**, *12*, 169−170.

(35) (a) Lee, C.; Yang, W.; Parr, R. G. *Phys. Rev. B: Condens. Matter Mater. Phys.* **1988**, *37*, 785−789. (b) Becke, A. D. *J. Chem. Phys.* **1993**, *98*, 1372−1377. (c) Becke, A. D. *J. Chem. Phys.* **1993**, *98*, 5648−5652.

(36) (a) Zhao, Y.; Truhlar, D. G. *Theor. Chem. Acc.* **2008**, *120*, 215−241. (b) Peverati, R.; Truhlar, D. G. *Philos. Trans. R. Soc., A* **2014**, *372*, 20120476.

(37) (a) Nyden, M. R.; Petersson, G. A. *J. Chem. Phys.* **1981**, *75*, 1843−1862. (b) Petersson, G. A.; Al-Laham, M. A. *J. Chem. Phys.* **1991**, *94*, 6081−6090. (c) Petersson, G. A.; Tensfeldt, T.; Montgomery, J. A. *J. Chem. Phys.* **1991**, *94*, 6091−6101. (d) Montgomery, J. A.; Ochterski, J. W.; Petersson, G. A. *J. Chem. Phys.* **1994**, *101*, 5900−5909.

(38) Moler, C.; Plesset, M. *Phys. Rev.* **1934**, *46*, 618−622.

DOI: 10.1021/acs.joc.5b02548
J. Org. Chem. XXXX, XXX, XXX−XXX

(39) (a) Dunning, T. H., Jr. *J. Chem. Phys.* **1989**, *90*, 1007−1023. (b) Woon, D. E.; Dunning, T. H., Jr. *J. Chem. Phys.* **1993**, *98*, 1358−1371.
(40) Bock, C. W.; Larkin, J. D. *Comput. Theor. Chem.* **2012**, *986*, 35−42.
(41) Bhat, K. L.; Markham, G. D.; Larkin, J. D.; Bock, C. W. *J. Phys. Chem. A* **2011**, *115*, 7785−7793.
(42) Monajemi, H.; Cheah, M. H.; Lee, V. S.; Zain, S. M.; Abdullah, W. A. T. W. *RSC Adv.* **2014**, *4*, 10505−10513.
(43) Smith, M. K.; Northrop, B. H. *Chem. Mater.* **2014**, *26*, 3781−3795.
(44) Zhao, Y.; Truhlar, D. G. *J. Chem. Theory Comput.* **2011**, *7*, 669−676.
(45) Burns, L. A.; Vazquez-Mayagoitia, A.; Sumpter, B. G.; Sherrill, C. D. *J. Chem. Phys.* **2011**, *134*, 084107.
(46) Jacquemin, D.; Perpète, E. A.; Ciofini, I.; Adamo, C.; Valero, R.; Zhao, Y.; Truhlar, D. G. *J. Chem. Theory Comput.* **2010**, *6*, 2071−2085.
(47) (a) Ess, D. H.; Houk, K. N. *J. Phys. Chem. A* **2005**, *109*, 9542−9553. (b) Gruner, V.; Khuong, K. S.; Leach, A. G.; Lee, P. S.; Bartberger, M. D.; Houk, K. N. *J. Phys. Chem. A* **2003**, *107*, 11445−11459.
(48) Larkin, J. D.; Bhat, G. D.; Markham, G. D.; Brooks, B. R.; Schaefer, H. F.; Bock, C. W. *J. Phys. Chem. A* **2006**, *110*, 10633−10642.
(49) Glendening, E. D.; Weinhold, F. *J. Comput. Chem.* **1998**, *19*, 610−627.
(50) Cordero, B.; Gómez, V.; Platero-Prats, A. E.; Revés, M.; Echeverría, J.; Cremades, E.; Barragán, F.; Alvarez, S. *Dalton Trans.* **2008**, 2832−2838.
(51) Frisch, M. J. et al. *Gaussian 09*, revision A.1, see Supporting Information.
(52) (a) Miertus, S.; Scrosso, E.; Tomasi, J. *Chem. Phys.* **1981**, *55*, 117−129. (b) Cossi, M.; Barone, V.; Cammi, R.; Tomasi, J. *Chem. Phys. Lett.* **1996**, *255*, 327−335.

DOI: 10.1021/acs.joc.5b02548
J. Org. Chem. XXXX, XXX, XXX−XXX